

Modelling of the Surface Morphology by Means of 2D Numerical Filters

Andrzej Golabczak, Andrzej Konstantynowicz
and Marcin Golabczak

Abstract When examining a surface machined by means of a repeatedly acting tool, especially a cyclically acting, as in the case of rotating machines, a characteristic pattern can be observed when analyzing the surface morphology. Such a pattern can be recognized as a characteristic symptom of the cooperation between the tool and the machined element, being usually in the tight contact. Obtaining any quantitative results evaluating this cooperation, demands establishing of the well suited mathematical model. In this paper a relationship is presented based on the numerical two-dimensional model filters of the quadrant type, acting on a square lattice representing surface. This appears to be an efficient numerical tool, providing a sufficient number of degrees of freedom and a fast execution, even though special measures have to be taken to assure their stability. The filters have been excited with simple stochastic processes simulating randomness of the abrasive machining at its basic level. The obtained results have been examined mainly by two methods: by using classical statistical analysis and by using the surface autocorrelation idea. This second method has been proven to be a good tool for the quantitative evaluation of the surface interaction during the machining process.

Keywords Surface texture · Stochastic processes · DSP · Spatial filtering

A. Golabczak (✉) · A. Konstantynowicz
Department of Production Engineering, Lodz University of Technology,
Stefanowskiego 1/15 Street, 90-924 Lodz, Poland
e-mail: andrzej.golabczak@p.lodz.pl

A. Konstantynowicz
e-mail: andrzej.konst@gmail.com

M. Golabczak
Institute of Machine Tools and Production Engineering, Lodz University of Technology,
Stefanowskiego 1/15 Street, 90-924 Lodz, Poland
e-mail: marcin.golabczak@p.lodz.pl

1 Stochastic Processes Basics

The term “stochastic process” term, often referred to as “random process” is a set of random variables (random varieties) representing the development of some system state over the independent variable X , very often representing time. In our case it represents the spatial variable. The exact mathematical definition is of less value for non-mathematicians and therefore we present in Fig. 1 a graphical representation of all the necessary elements and mutual dependencies. Two elements play the main role [7, 8]:

- the stochastic (random) mechanism generating the exact process value which is in our case simply the height of the roughness profile at the given X variable value which is in our case simply the point in physical space—depicted in green,
- assumed to be non-stochastic, a mechanism of the internal dependency between subsequent elementary events which in our case determine the similitude of roughness height in the juxtaposed spatial points—depicted in olive.

The first element is described by the probability density distribution, which is usually chosen from the small, widely used set. In this paper we will make primary use of the normal (Gaussian) distribution:

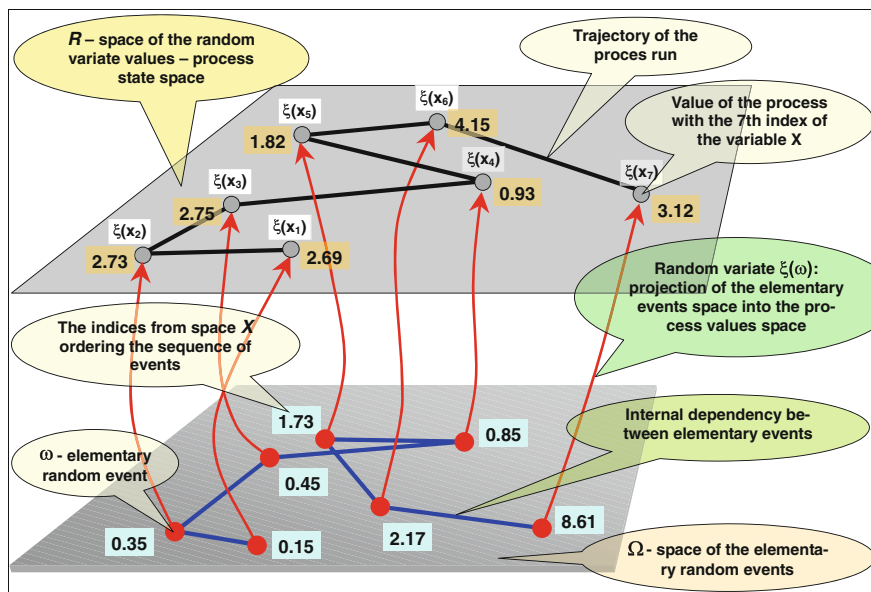


Fig. 1 The structure of mutual dependencies among the basic constituents of the “stochastic process”, as it will be used in the present paper

$$p(h) = \frac{1}{\sqrt{2\pi\sigma}} \exp\left(-\frac{(h - \mu)^2}{2\sigma^2}\right) \quad (1)$$

where μ —mean value of the variable h , and σ^2 —variance of the variable h .

The second distribution we will take into account is the logarithmic-normal distribution, called shortly “log-normal”, with the probability density:

$$p(h) = \frac{1}{\sqrt{2\pi} \cdot \sigma \cdot h} \exp\left(-\frac{(\ln(h) - \mu)^2}{2\sigma^2}\right) \quad (2)$$

where the description of variables is as previously stated. The relationship between the variable Y of the log-normal distribution and the N_0 variable of the normal distribution with $\mu = 0$, $\sigma^2 = 1$, is given by:

$$Y = \exp(k_\mu + k_\sigma \cdot N_0) \quad (3)$$

where

$$k_\mu = \ln\left(\frac{\mu_{\ln}^2}{\sqrt{\sigma_{\ln}^2 + \mu_{\ln}^2}}\right) \quad (4)$$

$$k_\sigma = \sqrt{\ln\left(1 + \frac{\sigma_{\ln}^2}{\mu_{\ln}^2}\right)} \quad (5)$$

For modelling purposes we have to be equipped with an efficient tool to generate variables with prescribed probability densities. The basic tool is the random number generator with uniform probability density, usually provided as embedded in the numerical software. Making use of simple mathematical rules related to the transformation of random variables we can use the following equation to get the first random variables N_1 with a normal probability distribution from random variables U_i with uniform probability distribution:

$$\begin{aligned} N_1 &= \sqrt{-2 \ln(U_1)} \cdot \cos(2\pi \cdot U_2) \\ N_2 &= \sqrt{-2 \ln(U_1)} \cdot \sin(2\pi \cdot U_2) \end{aligned} \quad (6)$$

This “twin generation” is very often used to obtain two “orthogonal” random variables, which, for our purpose, are the independent random variables.

2 Surface Modeling Using Digital Filters

In the classical division of the surface texture into three major components: shape, waviness and roughness [5], the application of digital filters for modelling allows us to successfully link two of these components: waviness and roughness. The way this is achieved is by using the aforementioned stochastic process theory and the application of digital filters to model the “internal dependency among spatial events”. This provides researchers with a tool to model the waviness, as seen in the olive mark in Fig. 1 [1, 2, 4]. Also the use of random signal generators to introduce the “unpredictability” element in modelling the roughness, as seen in Fig. 1 in light green [1, 7, 8], is also used to achieve this link. In this paper we have aimed at applying digital filters [2, 4, 6, 8], referring reader, for example, to the classical textbook, in the case [3] tools to accomplish it.

3 Digital Filtering Basics

So called digital filter are given by the numerical algorithm operating on samples of the signal, expressed as numbers. Usually one train of samples is referred to as the input—dependent signal, and the second train of pulses is referred to as the output—dependent signal. These signals could be ordered by integer indices. If there is one index—the signal is unidimensional, if two indices are necessary—the signal is two-dimensional. The object of our interest is a special type of two-dimensional digital filter described in terms of the recursive filter equation [2, 6], in the “spatial” domain:

$$h(i, j) = A_{w0} \cdot x_w(i) + A_{w1} \cdot h(i - 1, j) + A_{w2} \cdot h(i - 2, j) + A_{d0} \cdot x_d(j) + A_{d1} \cdot h(i, j - 1) + A_{d2} \cdot h(i, j - 2) \quad (7)$$

where

A_{w0}, A_{d0}	input amplitude coefficients: width and depth respectively,
$x_w(i), x_d(j)$	input excitation series: width and depth respectively,
A_{w1}, A_{w2}	width spatial memory coefficients for retarded samples,
A_{d1}, A_{d2}	depth spatial memory coefficients for retarded samples,
$h(i, j)$	output surface shape value for the point (i, j) .

The filter structure is depicted in Fig. 2. Input signals are marked with light green, initial conditions’ cells are marked with green and the active cells are marked with light yellow. In the active cells the filter equation is inscribed to show changes in indices. The dark green marked cells are involved during the calculation of the exemplary cell $(4, 4)$ value. The whole filter is organized on the 100×100 grid, which is not big enough for the targeted purpose, but is more than enough to show the filter behavior.

	X	0	1	2	3	4
Y	Xinput, Yinput	x(0)	x(1)	x(2)	x(3)	x(4)
0	y(0)	h(0,0)	h(1,0)	h(2,0)	h(3,0)	h(4,0)
1	y(1)	h(0,1)	h(1,1)	h(2,1)	h(3,1)	h(4,1)
2	y(2)	h(0,2)	h(1,2)	$h(2,2)=Aw0*x(2)+Aw1*h(1,2)+Aw2*h(0,2)+Ad0*y(2)+Ad1*h(2,1)+Ad2*h(2,0)$	$h(3,2)=Aw0*x(3)+Aw1*h(2,2)+Aw2*h(1,2)+Ad0*y(2)+Ad1*h(3,1)+Ad2*h(3,0)$	$h(4,2)=Aw0*x(4)+Aw1*h(3,2)+Aw2*h(2,2)+Ad0*y(2)+Ad1*h(4,1)+Ad2*h(4,0)$
3	y(3)	h(0,3)	h(1,3)	$h(2,3)=Aw0*x(2)+Aw1*h(1,3)+Aw2*h(0,3)+Ad0*y(3)+Ad1*h(2,2)+Ad2*h(2,1)$	$h(3,3)=Aw0*x(3)+Aw1*h(2,3)+Aw2*h(1,3)+Ad0*y(3)+Ad1*h(3,2)+Ad2*h(3,1)$	$h(4,3)=Aw0*x(4)+Aw1*h(3,3)+Aw2*h(2,3)+Ad0*y(3)+Ad1*h(4,2)+Ad2*h(4,1)$
4	y(4)	h(0,4)	h(1,4)	$h(2,4)=Aw0*x(2)+Aw1*h(1,4)+Aw2*h(0,4)+Ad0*y(4)+Ad1*h(2,3)+Ad2*h(2,2)$	$h(3,4)=Aw0*x(3)+Aw1*h(2,4)+Aw2*h(1,4)+Ad0*y(4)+Ad1*h(3,3)+Ad2*h(3,2)$	$h(4,4)=Aw0*x(4)+Aw1*h(3,4)+Aw2*h(2,4)+Ad0*y(4)+Ad1*h(4,3)+Ad2*h(4,2)$

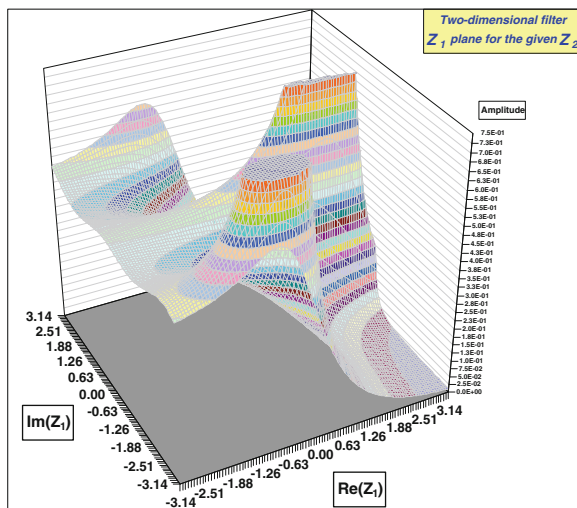
Fig. 2 Proposed filter structure with excitation and initial conditions setting. Cells marked with dark green color are involved during the calculating the exemplary cell value

For any digital filter it is essential to determine the conditions of stable work. The appropriate theoretical considerations could be found in positions [2, 6]. For the unidimensional filters they are relatively simple, but for two-dimensional filters it becomes more complicated. Even in the case of relatively simple filters proposed in this work, the exact numerical evaluation is complicated. Two theorems for the two-dimensional filter stability have been developed:

Theorem I *The two-dimensional filter with indefinite impulse responses (recursive), with the characteristics described by the rational polynomial complex function: $H(z_1, z_2) = \frac{N(z_1, z_2)}{D(z_1, z_2)}$ is stable when and only when $D(z_1, z_2) \neq 0$ for any z_1, z_2 for which $|z_1| \geq 1, |z_2| \geq 1$. This situation is illustrated in Fig. 3 for the exemplary filter we deal with further in this paper.*

Theorem II *The two-dimensional filter with rational polynomial characteristics, as in Theorem I, is stable when and only when the projection of the plane $|z_1| = 1$ onto the plane Z_2 , is equivalent the equation $D(z_1, z_2) = 0$, and is located entirely*

Fig. 3 The exemplary checking of the stability criterion I of the two-dimensional filter



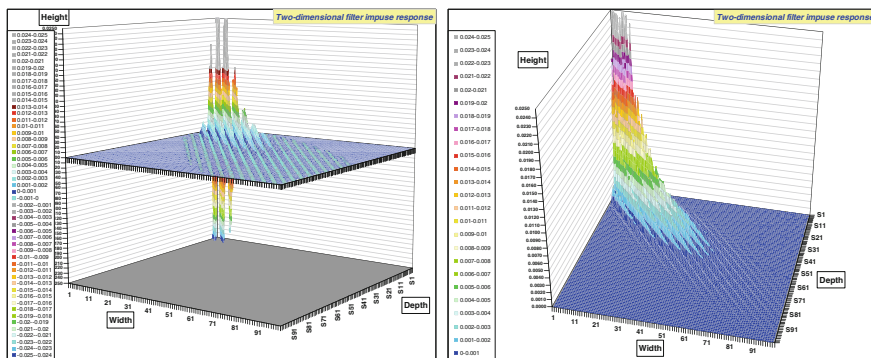


Fig. 4 The exemplary impulse response of the 2D filter (7) for the given coefficients: two different views

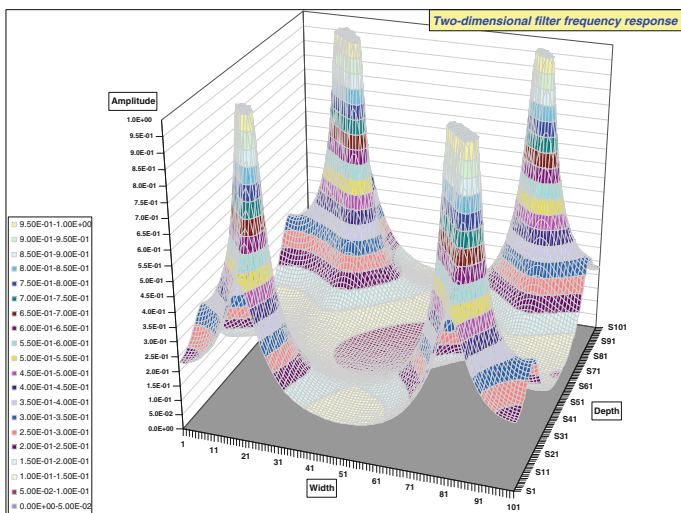


Fig. 5 The exemplary filter impulse response in the frequency domain

inside the plane $|z_2| \geq 1$, and, the projection $D(z_1, z_2) = 0$ does not reflect any point from the plane $|z_1| \geq 1$ onto the point $|z_2| = 0$.

The impulse response at Fig. 4 has been charted for the exemplary filter coefficients (Fig. 5):

$A_{w0} = 0.100000$	$A_{w1} = 0.375000$	$A_{w2} = -0.425000$
$A_{d0} = 0.100000$	$A_{d1} = 0.575000$	$A_{d2} = -0.395000$
Exemplary grid step	$\Delta w = 1 \mu\text{m}, \Delta d = 1 \mu\text{m}$	
Dimension of the grid	$N \times N = 100 \times 100$	

The frequency response of the filter (7) is given as the Z-transformation of the filter impulse response taken at the unitary circle at the complex z-plane, i.e. for $z_w = \exp(j\omega_w \Delta w)$, $z_d = \exp(j\omega_d \Delta d)$:

$$F(\omega_w, \omega_d) = \frac{A_{w0} + A_{d0}}{1 - A_{w1} \cdot e^{-j\omega_w \Delta w} - A_{w2} \cdot e^{-2j\omega_w \Delta w} - A_{d1} \cdot e^{-j\omega_d \Delta d} - A_{d2} \cdot e^{-2j\omega_d \Delta d}} \tag{8}$$

where

$\Delta w, \Delta d$ spatial sampling step of the filter grid: width and depth respectively,
 ω_w, ω_d spatial frequencies: width and depth respectively, other coefficients as in Eq. (7).

4 Numerical Results

The numerical simulations we have performed, have aimed at demonstrating the usability and functionality of the proposed filter in generation surfaces widely occurring in surface machining at different stages of mechanical accuracy, performed with using very different tools ranged from raw milling to abrasive cloth polishing. The exemplary excitation source for surfaces depicted in Figs. 6 and 7

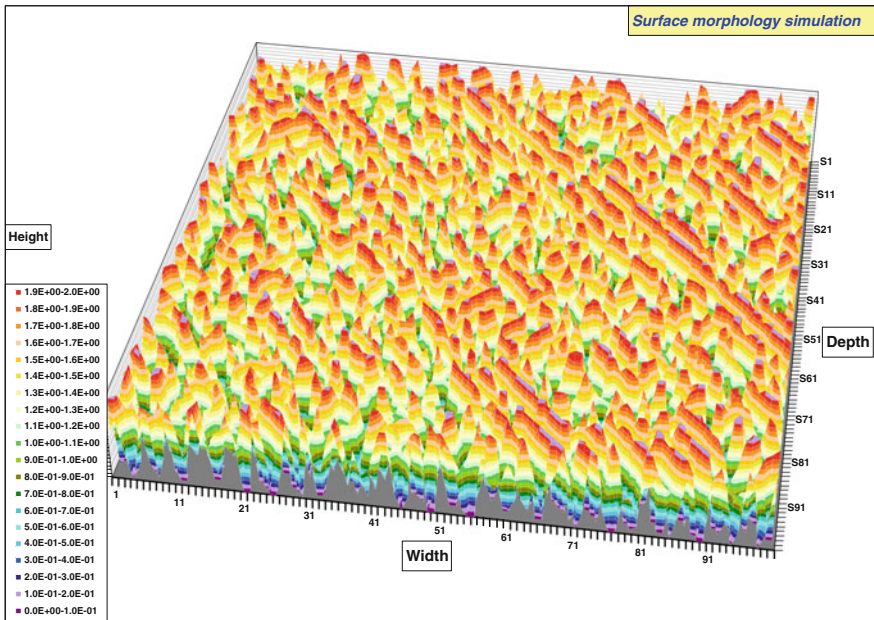


Fig. 6 Surface texture generated by using the filter of the impulse response depicted in Fig. 4

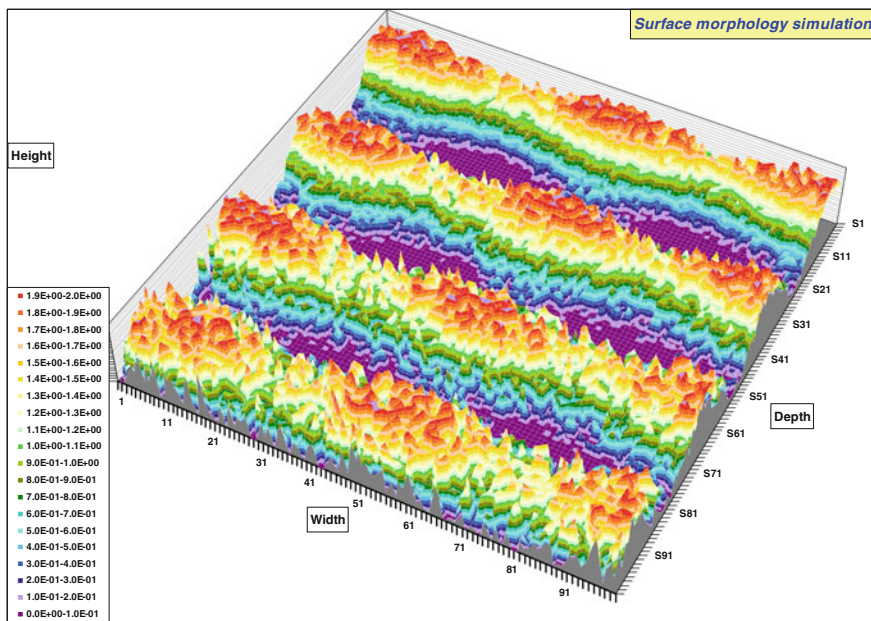


Fig. 7 Surface texture generated by using the filter of another impulse response, more suitable for modelling of the rotating machine rough machining

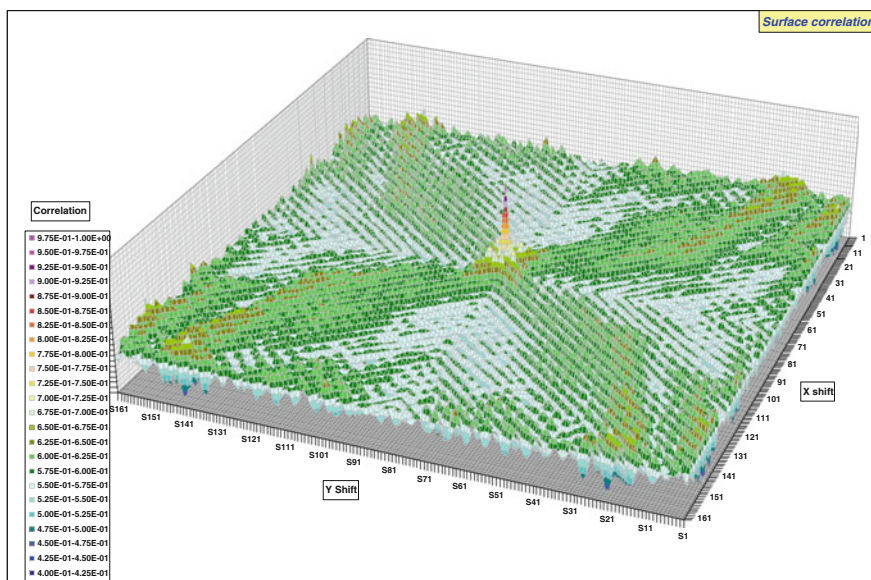


Fig. 8 Two-dimensional correlation function for the surface from Fig. 6

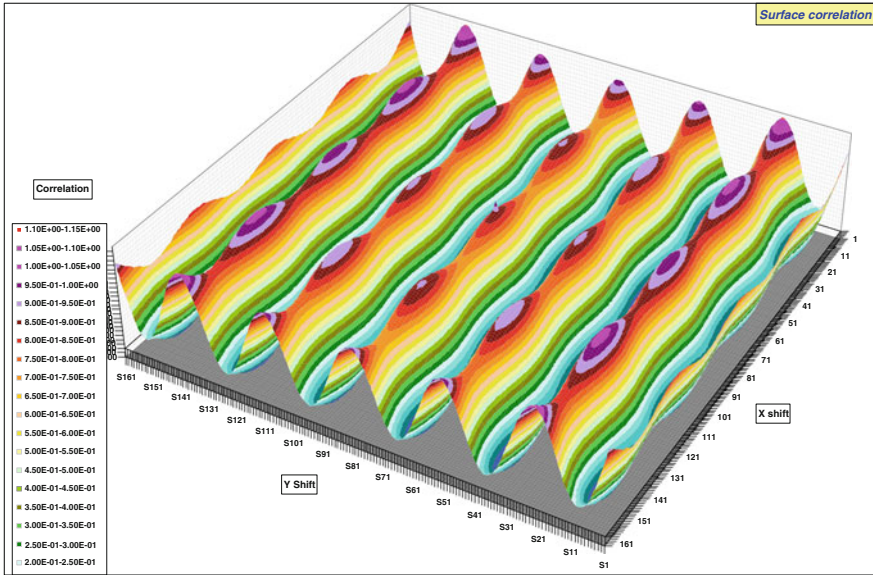


Fig. 9 Two-dimensional correlation function for the surface from Fig. 7

were Gaussian random number generators with variance parameters: $A_w = 1.00$, $A_d = 0.01$ respectively. The referenced surfaces exemplify abrasive cloth polishing and raw milling respectively.

For to bring out the proposed filter span of use, the two-dimensional autocorrelation function:

$$R(m, n) = \frac{1}{(N - m) \cdot (N - n)} \sum_{i=1}^{N-m} \sum_{j=1}^{N-n} h(i, j) \cdot h(m + i, n + j) \tag{9}$$

has also been calculated for the surfaces from Figs. 6 and 7 and depicted in Figs. 8 and 9.

5 Conclusions

The two-dimensional filter presented in this work, although relatively simple in its class, proved to be an efficient tool in generating surface textures from the broad range of textures encountered in the surface machining to different grades of finishing and performed with different tools. In our further works we'll tend to apply it to modelling of the machined surfaces we currently deal with: AZ31 magnesium alloy, Ti6Al4V titanium alloy and X38CrMoV5-1 steel.

References

1. Box G, Jenkins G, Reinsel G (2008) Time series analysis: forecasting and control. Prentice Hall, Englewood Cliffs
2. Griffith DA (2003) Spatial autocorrelation and spatial filtering. Springer, Berlin
3. Knuth D (1968) The art of computer programming. Addison-Wesley, Boston
4. Lloyd Ch (2010) Local models for spatial analysis. CRC Press, Boca Raton
5. Petropoulos G, Pandazaras C, Davim J (2010) Surface texture characterization and evaluation related to machining. In: Davim J (ed) Surface integrity in machining. Springer, Berlin
6. Rabiner L, Gold B (1975) Theory and application of digital signal processing. Prentice-Hall, Englewood Cliffs
7. Taylor H, Karlin S (1998) An introduction to stochastic modeling. Academic Press, Waltham
8. Van Kampen N (1992) Stochastic processes in physics and chemistry. Elsevier, Amsterdam